Linear Bis(perfluoroalkyl) Complexes of Nickel Bipyridine

Yoshitaka Yamaguchi,[†,‡] Hiromi Ichioka,[†] Axel Klein,[§] William W. Brennessel,[‖] and David A. Vicic*,[†]

[†]Department of Chemistry, University of Hawaii, 2545 McCarthy Mall, Honolulu, Hawaii 96822, United States
[‡]Department of Advanced Materials Chemistry, Graduate School of Engineering, Yokohama National University, Tokiwadai 79-5, Hodogaya-ku, Yokohama, 240-8501, Japan
[§]Universität zu Köln, Institut für Anorganische Chemie, Greinstrasse 6, D-50939 Köln, Germany
[‖]The X-ray Crystallographic Facility, Department of Chemistry, University of Rochester, Rochester, New York 14627, United States

Ⓢ Supporting Information

ABSTRACT: Three new complexes were prepared: $[(dtbpy)-Ni(CF_3)_2]$ (**1**), $[(dtbpy)Ni(CF_2CF_3)_2]$ (**2**), and $[(dtbpy)Ni-(CH_3)_2]$ (**3**) (dtbpy = 4,4′-di-*tert*-butyl-2,2′-bipyridine). Remarkable differences in the structure, electronics, reactivity, and absorption of visible light for the alkyl versus perfluoroalkyl complexes were observed and are detailed in this report.
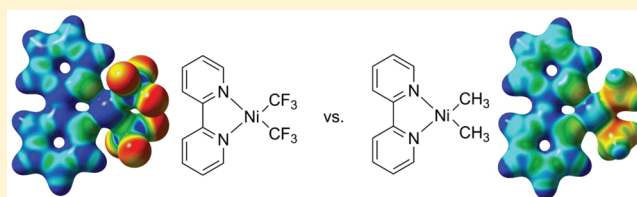
INTRODUCTION

Nickel bipyridine complexes have played a significant role in synthetic chemistry. Much of the fundamental information regarding reductive elimination processes,[1−10] redox events,[4,7,11−14] insertion reactions,[15−28] polymer synthesis,[29−40] and electrocatalytic couplings[41−45] using nickel comes from studies initiated with complexes bearing the bipyridine ligand. With the explosion of interest in synthesizing organic molecules bearing perfluoroalkyl functional groups,[46−57] we became interested in preparing nickel bipyridine complexes bearing two perfluoroalkyl ligands in order to compare and contrast the reactivity with that known for nickel bipyridine dialkyl complexes. The only two known fluoroalkyl complexes of a nickel bipyridine framework, however, are metallacycles that are both prepared by oxidative cyclization of fluorinated olefins.[58−60] There has been no report on the preparation of linear fluoroalkyl complexes based on nickel bipyridine, and these are the type of complexes that are needed to study processes most relevant to synthetic applications, such as reductive elimination.

Another motivation for preparing nickel bipyridine bis-(perfluoroalkyl) complexes is that they may offer an internal spectroscopic handle to further study the electronic properties of perfluoroalkyl ligands. Square-planar nickel complexes of 2,2′-bipyridine (or derivatives) show intense metal-to-ligand charge transfer bands in the visible part of the electronic absorption spectra. A detailed study of the UV−vis spectra of the closely related complexes $[(bpy)Ni(CH_3)_2]$ (**4**), $[(bpy)-Ni(Mes)_2]$ (**5**), and $[(bpy)Ni(Mes)Br]$ (**6**) (Mes = mesityl = 2,4,6-trimethylphenyl) has recently been reported,[61] and while the low-energy transitions responsible for the long-wavelength absorptions of **5** and **6** have distinct contributions from the aryl coligand, the $[(bpy)Ni(CH_3)_2]$ complex exhibited almost pure metal (d) to ligand (π^*) charge-transfer transitions. With this in mind, we were quite interested to see how the optical spectrum would change upon fluorination of the alkyl coligands, as changes would directly reflect the electronic properties of the metal and fluoroalkyl groups.

It is already known that the fluoroalkyl functional group can confer special electronic properties to a molecule at both the local and global levels. At the global level, much evidence has been reported describing the fluoroalkyl group as a classic electron-withdrawing group. For instance, competitive electro-philic aromatic substitution reactions of He^3H^+ among trifluorotoluene, benzene, and toluene provided the following relative rates for tritium incorporation: trifluorotoluene, 0.45; benzene, 1.00; toluene, 2.1.[62] High CO stretching frequencies have also been reported for metal complexes bearing both a carbonyl group and a CF_3 group;[63,64] the CO stretch for $[AuCl(CO)]$ appears at 2162 cm^{-1}, while that for $[Au(CF_3)-CO)]$ appears at 2180 cm^{-1}.[63] Moreover, experiments show that many organic[65] and organometallic[66] complexes bearing fluoroalkyl groups are more difficult to oxidize electrochemi-cally than their nonfluorinated counterparts. At the local level, however, perfluoroalkyl groups may confer properties that are often observed with electron-donating groups. For instance, high-valent metal complexes can often be stabilized with perfluoroalkyl ligands.[67,68] Metal−CF_3 complexes also display trans-influencing properties quite similar to those of their metal−CH_3 counterparts.[66,69] Finally, density functional theory (DFT) studies suggest that atoms directly attached to a CF_3 group in both aromatic and organometallic complexes can bear a less positive calculated charge than their nonfluorinated analogues.[70]

In order to assess how fluorination of the organic coligands affects the nickel bipyridine system, we have decided to prepare complexes **1**–**3**. Remarkable differences in the structure, electronics, reactivity, and absorption of visible light for the alkyl versus perfluoroalkyl complexes were observed and are detailed below.

■ RESULTS AND DISCUSSION

The fluoroalkyl complexes **1** and **2** were prepared by reacting [(dme)NiBr$_2$] (dme = 1,2-dimethoxyethane) with an excess of cesium fluoride and Me$_3$SiCF$_3$ in a DMF/THF solvent mixture (eq 1). The order of addition is important because formation of

excess Me$_3$Si-R$_f$
excess CsF
DMF/THF, RT

same as above
CH$_2$Cl$_2$

(1)

1, R$_f$ = CF$_3$
2, R$_f$ = CF$_2$CF$_3$

+ **2**

7, R$_f$ = CF$_2$CF$_3$

(trace)
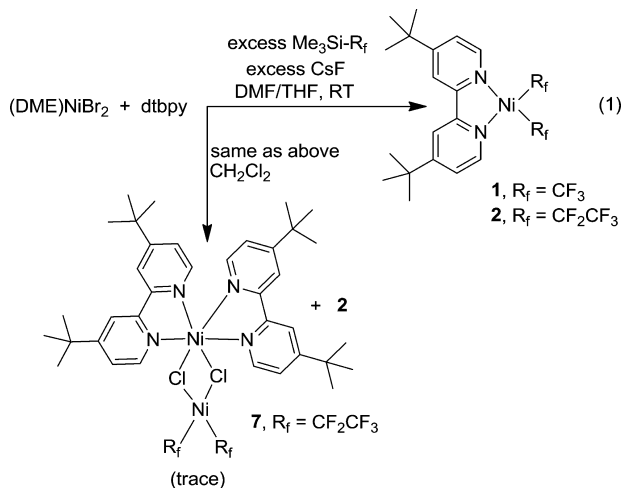
the product is competitive with formation of the CF$_3$ adduct of DMF.[71] We have independently determined that the CF$_3$ adduct of DMF is ineffective at transmetalating the nickel bipyridine precursor. Yellow crystals of **1** may be obtained from precipitating the reaction mixtures using THF and pentane, and the ORTEP diagram is shown in Figure 1. A striking feature of the molecular geometry of **1** is the large distortion from square planarity. The trans nitrogen−nickel−carbon bond angles were found to be 159.7(2) and 165.1(2)°, far from the idealized 180°. Steric interactions of the fluorines with the 6- and 6′-

hydrogens of the bipyridine ligand are most likely responsible for this distortion (see below). The nickel−carbon distances in **1** were Ni(1)−C(1) = 1.872(6) Å and Ni(1)−C(2) = 1.883(6) Å, substantially shorter than the nickel−carbon bond lengths found in the nonfluorinated analogue [(bpy)Ni(CH$_3$)$_2$], which have a distance of 1.923(4) Å.[72] The nickel−nitrogen bond lengths in **1** are asymmetric, with bond distances of 1.983(4) and 1.955(5) Å. For comparison, the nickel−nitrogen bond lengths in [(bpy)Ni(CH$_3$)$_2$] were found to be 1.965(3) Å.[72] Thus, at first glance the bond lengths are consistent with the trans-influencing properties of the trifluoromethyl group being on par with that of the methyl in these derivatives of nickel. However, the large structural distortions of the CF$_3$ complex relative to the CH$_3$ counterpart may limit meaningful interpretation. Despite the distorted geometry, complex **1** is thermally stable (unlike the dimethyl derivative, which loses ethane upon gentle warming) and can be exposed to air for weeks without noticeable decomposition.

Orange crystals of the air-stable bis-C$_2$F$_5$ complex **2** could similarly be obtained by the procedure outlined in eq 1, and X-ray analysis of these crystals reveals an even larger distortion from square planarity (Figure 2). Both of the trans carbon−nickel−nitrogen bond angles were found to be 152.2(2)°, and the nickel−carbon distances were found to be substantially longer than those in **1** at 1.910(6) and 1.911(6) Å. Care with solvent choice must be taken when preparing the bis-(perfluoroalkyl) complexes, for if the reaction described in eq 1 (using Me$_3$SiCF$_2$CF$_3$) was performed in CH$_2$Cl$_2$, trace amounts of the bridging chloride complex **7** could be obtained. The nickel−carbon bond lengths in **7** were found to be 1.930(5) and 1.919(6) Å, considerably longer than those found in complex **1** but similar to those in **2**. Figure 3 shows that the nickel center bearing the perfluoroethyl groups in **7** now adopts a far less distorted square-planar arrangement than that observed in **2**, likely due to the absence of steric interactions with the bipyridine hydrogens as described for **2**.

The colors of the new metal complexes deserve mention. Crystals and solutions of **1** are yellow, and those of **2** are orange, whereas that of the nonfluorinated [(dtbpy)Ni(CH$_3$)$_2$] (**3**) derivative is dark green (similar to the known [(bpy)Ni-(CH$_3$)$_2$]).[72] The experimental visible spectra are shown in
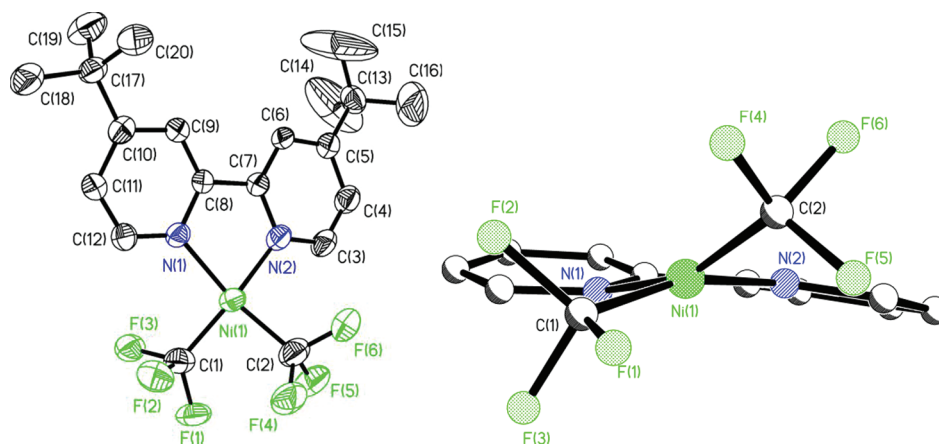
Figure 1. (left) ORTEP diagram of [(dtbpy)Ni(CF$_3$)$_2$] (**1**). Ellipsoids are shown at the 50% level. Hydrogen atoms are removed for clarity. Selected bond lengths (Å): Ni(1)−N(1), 1.983(4); Ni(1)−N(2), 1.955(5); Ni(1)−C(1), 1.872(6); Ni(1)−C(2), 1.883(6). Selected bond angles (deg): N(1)−Ni(1)−N(2), 82.01(19); N(1)−Ni(1)−C(1), 97.1(2); N(1)−Ni(1)−C(2), 159.7(2); N(2)−Ni(1)−C(1), 165.1(2); N(2)−Ni(1)−C(2), 95.6(2); C(1)−Ni(1)−C(2), 90.3(3). (right) Ball and stick diagram of **1** showing the distortion of square planarity. *tert*-Butyl groups and all hydrogens are removed for clarity.
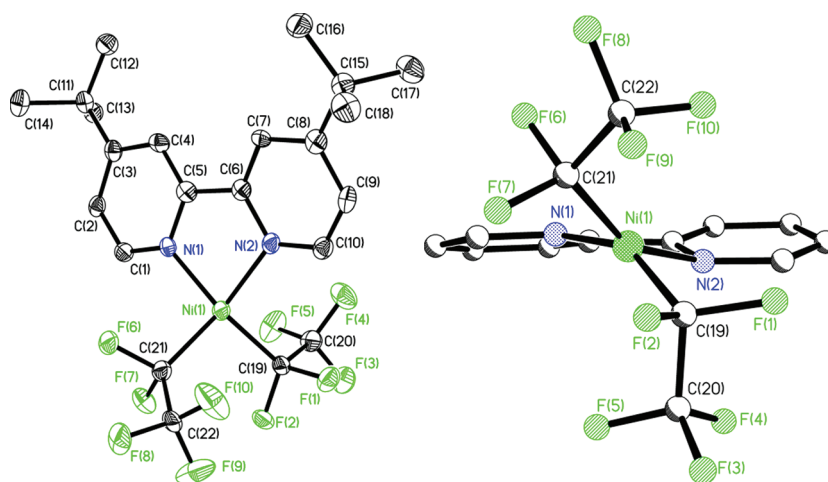
Figure 2. (left) ORTEP diagram of $[(\text{dtbpy})\text{Ni}(\text{CF}_2\text{CF}_3)_2]$ (**2**). Ellipsoids are shown at the 50% level. Hydrogen atoms are removed for clarity. Selected bond lengths (Å): Ni(1)−C(21), 1.910(6); Ni(1)−C(19), 1.911(6); Ni(1)−N(1), 1.941(5); Ni(1)−N(2), 1.960(5); C(19)−C(20), 1.530(9); C(21)−C(22), 1.551(9). Selected bond angles (deg): C(21)−Ni(1)−C(19), 94.0(3); C(21)−Ni(1)−N(1), 96.7(2); C(19)−Ni(1)−N(1), 152.2(2); C(21)−Ni(1)−N(2), 152.2(2); C(19)−Ni(1)−N(2), 100.0(2); N(1)−Ni(1)−N(2), 81.8(2). (right) Ball and stick diagram of **2** showing the distortion of square planarity. *tert*-Butyl groups and all hydrogens are removed for clarity.
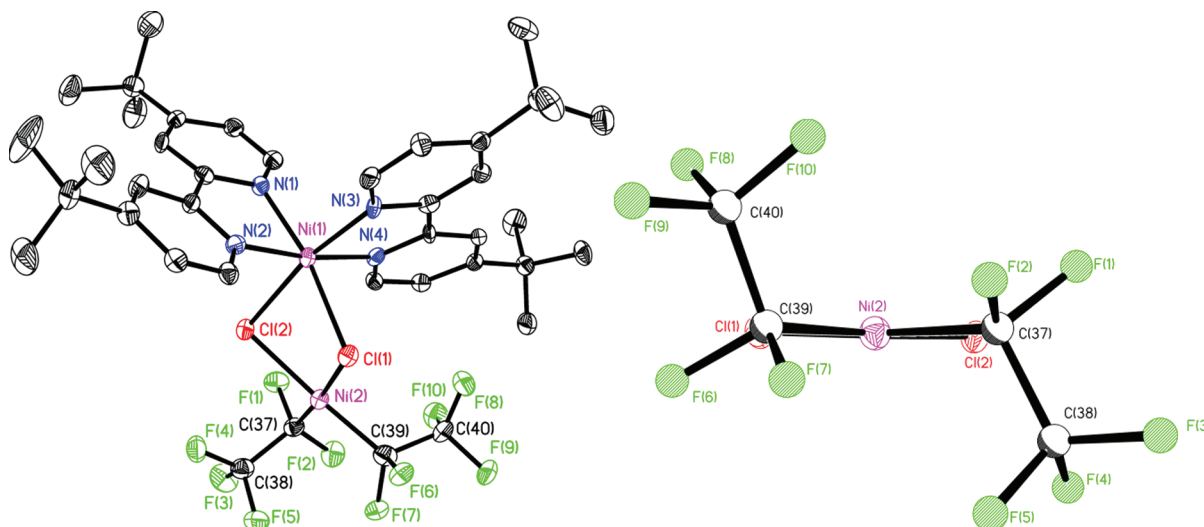
Figure 3. (left) ORTEP diagram of **7**. Ellipsoids are shown at the 50% level. Hydrogen atoms are removed for clarity. Selected bond lengths (Å): Ni(1)−N(3), 2.047(4); Ni(1)−N(2), 2.053(5); Ni(1)−N(4), 2.057(4); Ni(1)−N(1), 2.080(4); Ni(1)−Cl(2), 2.4258(15); Ni(1)−Cl(1), 2.4269(15); Ni(2)−C(39), 1.919(6); Ni(2)−C(37), 1.930(5); Ni(2)−Cl(2), 2.2746(15); Ni(2)−Cl(1), 2.2753(15). Selected bond angles (deg): N(3)−Ni(1)−N(2), 95.78(17); N(3)−Ni(1)−N(4), 79.66(17); N(2)−Ni(1)−N(4), 172.02(18); N(3)−Ni(1)−N(1), 98.75(17); N(2)−Ni(1)−N(1), 78.43(17); N(4)−Ni(1)−N(1), 95.69(17); N(3)−Ni(1)−Cl(2), 169.43(13); N(2)−Ni(1)−Cl(2), 89.02(13); N(4)−Ni(1)−Cl(2), 96.58(13); N(1)−Ni(1)−Cl(2), 91.44(12); N(3)−Ni(1)−Cl(1), 91.52(13); N(2)−Ni(1)−Cl(1), 98.01(13); N(4)−Ni(1)−Cl(1), 88.70(13); N(1)−Ni(1)−Cl(1), 169.40(13); Cl(2)−Ni(1)−Cl(1), 78.46(5); C(39)−Ni(2)−C(37), 93.2(2); C(39)−Ni(2)−Cl(2), 175.88(18); C(37)−Ni(2)−Cl(2), 90.75(17); C(39)−Ni(2)−Cl(1), 91.15(17); C(37)−Ni(2)−Cl(1), 175.13(18); Cl(2)−Ni(2)−Cl(1), 84.83(5); Ni(2)−Cl(1)−Ni(1), 90.72(5); Ni(2)−Cl(2)−Ni(1), 90.77(5). (right) Ball and stick diagram showing the square-planar coordination around Ni2.

Figure 4. The bis-CH_3 derivative shows two intense and broad absorption bands at 402 and 640 nm. Deconvolution of the known $[(\text{bpy})\text{Ni}(\text{CH}_3)_2]$ spectrum by time-dependent DFT (TD-DFT) showed that these low-energy transitions are purely MLCT (MLCT = metal-to-ligand charge transfer) in character.[61] The most striking feature of the spectra of the bis(perfluoroalkyl) complexes is that the low-energy absorption bands from 600 to 700 nm for the bis(perfluoroalkyl) complexes **1** and **2** were found to be suppressed, but the band centered at ∼370 nm was still present. The likely explanation is that the corresponding transitions for these bands are of very mixed character, including contributions from the Ni−CF_3 σ bonds. Thus, while a general view on the

absorption spectra would suggest similar transitions for both the CF_3 and CH_3 complexes with a marked blue shift for the CF_3 derivative and a dramatic loss of intensity for the low-energy charge transfer absorption, a closer look reveals that only the high-energy $\pi-\pi^*$ transitions are of similar character, while the long-wavelength charge transfer absorptions differ largely in character, when replacing CH_3 by CF_3. The main differences seem to arise from the involvement of orbitals with CF_3 contributions (or Ni−CF_3) for $[(\text{bpy})\text{Ni}(\text{CF}_3)_2]$, while the CH_3 coligand does not contribute to the transitions of $[(\text{bpy})\text{Ni}(\text{CH}_3)_2]$. Another possible explanation for the absence of a low-energy band is that the experimentally observed geometric distortions are disabling efficient Ni (3d)−
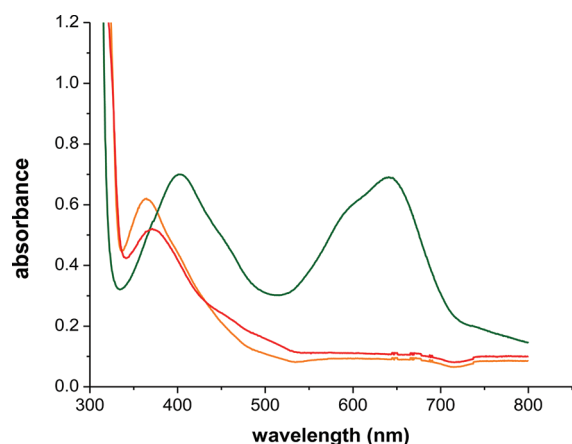
Figure 4. Experimental UV−vis spectra in THF: complex **1** (orange), ε_{364} = 2484 M^{-1} cm^{-1}; complex **2** (red), ε_{372} = 2078 M^{-1} cm^{-1}; complex **3** (green), ε_{402} = 2800 M^{-1} cm^{-1}.

bpy (π*) overlap. A full TD-DFT analysis of the molecular orbital contributions to the absorption energies of the bis(perfluoroalkyl) complexes is needed to thoroughly understand and describe the electronic spectra, and such studies will be reported in due course.

With the molecular coordinates of the metal centers in these new perfluoroalkyl complexes in hand, DFT analyses were performed using a truncated bipyridine ligand. Figure 5 shows a
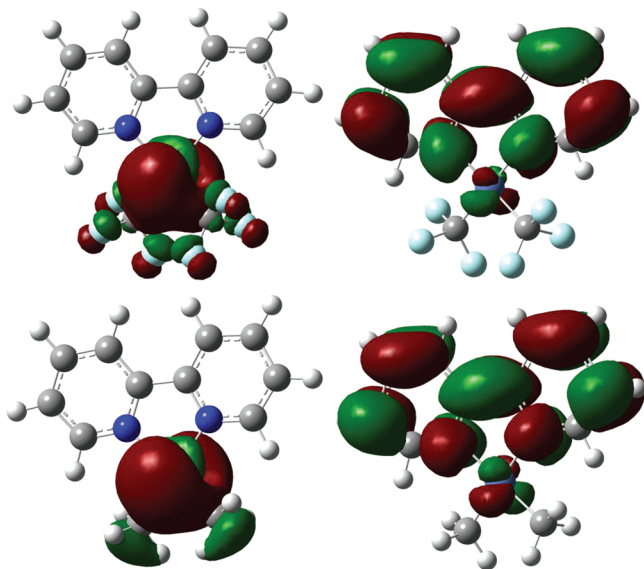
Figure 5. Calculated HOMO (left) and LUMO (right) of [(bpy)Ni-(CF$_3$)$_2$] (top) and [(bpy)Ni(CH$_3$)$_2$] (bottom).

graphical representation of the highest occupied molecular orbital (HOMO) and the lowest unoccupied molecular orbital (LUMO) of [(bpy)Ni(CH$_3$)$_2$] and [(bpy)Ni(CF$_3$)$_2$], and Table 1 shows calculated versus experimental bond lengths and angles. The distinguishing features of the molecular orbitals are that the HOMO of each is largely metal-centered and the LUMO of each is largely ligand-centered. An analysis of the charge distribution in these new complexes was also performed, and Figure 6 shows that fluorination has the known effect of decreasing the charge on the atom attached to the fluoroalkane (namely, nickel). Fluorination also has the effect of dramatically
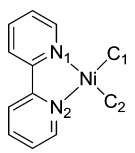
"redistributing" the charge in the molecules. For instance, in the bis-CH$_3$ complex, the carbon atoms of the methyl group are negatively charged, whereas in the bis(perfluoroalkyl) complexes the carbon atoms bound to the metal are positively charged with the negative charge residing primarily on the fluorine atoms.

The nickel center in [(bpy)Ni(CH$_3$)$_2$] has a calculated charge of 0.59e, higher than that of [(bpy)Ni(CF$_3$)$_2$] at 0.43e. This bears importance in discussions of the electronic spectra. If the nickel center in [(bpy)Ni(CF$_3$)$_2$] bears a less positive charge, why then are the experimental visible absorption energies higher than those observed for the bis-CH$_3$ complex? A comparison of the calculated molecular orbital energies of the two complexes offers some insight. Figure 7 reveals that both the HOMO and the LUMO of the bis-CF$_3$ complex are largely stabilized over the corresponding orbitals of the bis-CH$_3$ derivative.[73] However, because the stabilization of the HOMO for the bis-CF$_3$ derivative is almost 2 times larger than the stabilization of the LUMO, charge-transfer transitions for the bis-CF$_3$ derivative are expected to lie higher in energy. Precedence for significant stabilization of the HOMO by fluoroalkyl groups comes from photoelectron and computational studies by Puddephatt and co-workers, who showed that the d orbitals of [(COD)Pt(CF$_3$)$_2$] were all stabilized relative to [(COD)Pt(CH$_3$)$_2$].[74] Grushin and co-workers have also noted that the calculated d orbital energy levels in [(H$_3$P)$_3$Rh-(CF$_3$)] are 9−15 kcal/mol more stable than in the [(H$_3$P)$_3$Rh-(CH$_3$)] derivative.[70] It is also of note that the stabilization of the HOMO by fluorine in organometallic chemistry has been seen in other ligands in addition to perfluoroalkyl groups. Hughes noted that the energies of the top three occupied MOs of ruthenocenes, as measured by gas-phase photoelectron spectroscopy, were all lower for a derivative containing a fluorinated cyclopentadienyl ligand than for a nonfluorinated derivative.[75,76] The HOMO stabilization also explains the observed electrochemical features in these new complexes. The bis-CF$_3$ complex **1** was found to exhibit one quasi-reversible oxidation with an oxidation peak potential at +0.90 V vs Fc$^+$/Fc in THF solution. Complex **1** is far more difficult to oxidize than the bis-CH$_3$ derivative **3**, which exhibits an irreversible oxidation at −0.60 V vs Fc$^+$/Fc in THF solution. This ΔE_{ox} value of 1.5 V is the largest we have thus far observed experimentally with nickel.[66]

In summary, we have been able to prepare new bis-(perfluoroalkyl) complexes of nickel bearing a bipyridine coligand. The perfluoroalkyl complexes, unlike the non-fluorinated dialkyl derivatives, are thermally quite stable, despite extremely distorted square-planar geometries. DFT analysis of both [(bpy)Ni(CF$_3$)$_2$] and [(bpy)Ni(CH$_3$)$_2$] predicts a large stabilization of the HOMO for the bis-CF$_3$ complex, which is consistent with the observed stability, oxidation potential, and optical spectrum relative to those for the bis-CH$_3$ complex. The data also further highlight the fact that, when comparing alkyl versus fluoroalkyl ligands, calculated atomic charges are most meaningfully discussed in combination with global molecular orbital energy considerations.

■ EXPERIMENTAL SECTION

General Considerations. All manipulations were performed using standard Schlenk and high-vacuum techniques or in a nitrogen-filled glovebox. Solvents were distilled from Na/benzophenone or CaH$_2$. DMF was distilled over BaO under reduced pressure. All reagents were used as received from commercial vendors, unless otherwise noted.

Table 1. Comparison of Experimental Bond Lengths in 1 and 2 to Those in $[(bpy)Ni(CF_3)_2]$ and $[(bpy)Ni(C_2F_5)_2]$

bond length or angle	complex 1 (exptl)	$[(bpy)Ni(CF_3)_2]$ (calcd)	complex 2 (exptl)	$[(bpy)Ni(C_2F_5)_2]$ (calcd)
Ni−C1	1.872(6)	1.899	1.910(6)	1.919
Ni−C2	1.883(6)	1.899	1.911(6)	1.930
Ni−N1	1.955(5)	1.995	1.941(5)	2.007
Ni−N2	1.983(4)	1.996	1.960(5)	1.999
N1−Ni−C1	97.1(2)	95.7	96.7(2)	98.7
N1−Ni−C2	159.7(2)	162.7	152.2(2)	152.4
N2−Ni−C2	95.6(2)	95.9	100.0(2)	98.2
N2−Ni−C1	165.1(2)	162.1	152.2(2)	154.9
N1−Ni−N2	82.01(19)	81.5	81.8(2)	81.0
C1−Ni−C2	90.3(3)	91.9	94.0(3)	93.3
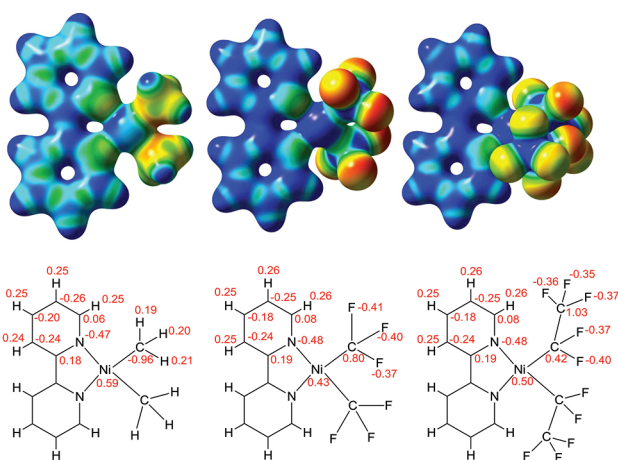
Figure 6. (top) DFT-calculated electrostatic surface potentials of complexes $[(bpy)Ni(CH_3)_2]$, $[(bpy)Ni(CF_3)_2]$, and $[(bpy)Ni(CF_2CF_3)_2]$. Red indicates regions of negative charge, while blue indicates regions of positive charge: isovalue, 0.02; density, 0.04. (bottom). Calculated natural atomic charge distributions from a Natural Bond Orbital[77] analysis.

Elemental analyses were performed by Columbia Analytical Services. ^{1}H NMR spectra were recorded at ambient temperature (unless otherwise noted) on a Varian Oxford 300 MHz spectrometer and referenced to residual proton solvent signals. ^{13}C NMR spectra were recorded on the Varian Oxford spectrometer operating at 75 or 126 MHz and were referenced to solvent signals. ^{19}F spectra were recorded on the Varian Oxford spectrometer operating at 282 MHz and were referenced to α,α,α-trifluorotoluene as an internal standard (δ −63.7). UV−vis absorption spectra were recorded in 1 cm quartz cells using a Varian Cary 50 Scan photospectrometer. Cyclic voltammetry experiments were performed using 10 mM metal complex and 100 mM electrolyte ($[Bu_4N][BAr_4]$, where Ar = C_6F_5) in THF solvent and referenced to Ag/AgCl and calibrated to internally added decamethylferrocene (202 mV in THF). After calibration, peak potentials were referenced vs ferrocene (629 mV in THF).[78]

Preparation of $[(dtbpy)Ni(CF_3)_2]$ (1). A 100 mL round-bottom flask was charged with $[NiBr_2(dme)]$ (0.202 g, 0.65 mmol), dtbpy (0.201 g, 0.75 mmol), and THF (10 mL). Within a few minutes, the solution had turned green. After stirring at room temperature for 10 min, DMF (5 mL) and CsF (0.451 g, 2.97 mmol) were added to the flask. After 5 min, a DMF solution of Me_3SiCF_3 (0.430 g, 3.02 mmol in 3 mL of DMF) was added dropwise. The reaction mixture was stirred overnight, and then the volatiles were removed under reduced
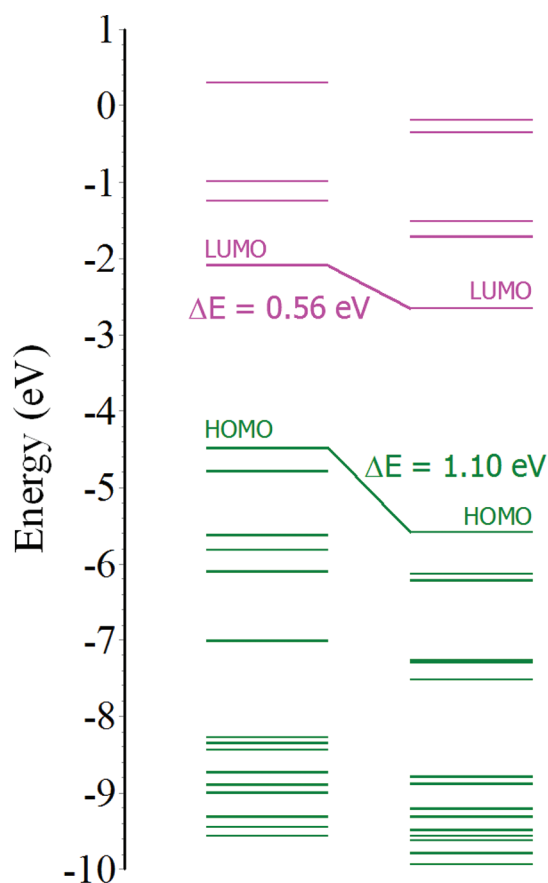
Figure 7. Calculated molecular orbital energy levels in the energy range −10.0 to 1.00 eV showing occupied (green) and unoccupied (pink) MOs of $[(bpy)Ni(CF_3)_2]$ (right) and $[(bpy)Ni(CH_3)_2]$ (left).

pressure. The residue was redissolved in Et_2O (40 mL), and the solution was passed through a Celite pad on a glass filter. After the volatiles were removed, the residual solid was washed with hexane (10 mL × 2) and dried in vacuo to yield $[(dtbpy)Ni(CF_3)_2]$ as a yellow powder (0.033 g, 0.071 mmol, 11%). Suitable single crystals for X-ray analysis were obtained by recrystallization from equal amounts of THF and pentane at −35 °C. ^{1}H NMR (300 MHz, THF-d_8): δ 8.60 (d, J = 6.0 Hz, 2H, dtbpy), 8.19 (s, 2H, dtbpy), 7.66 (d, J = 6.0 Hz, 2H, dtbpy), 1.41 (s, 18H, CH_3). ^{13}C{^{1}H} NMR (126 MHz, THF-d_8): δ 165.5 (s, dtbpy), 155.8 (s, dtbpy), 153.1 (s, dtbpy), 131.3 (quint, $^1J_{CF}$ = 369.1 Hz, CF_3), 124.5 (s, dtbpy), 119.2 (s, dtbpy), 36.3 (s,

C(CH$_3$)$_3$), 30.3 (s, C(CH$_3$)$_3$). ^{19}F NMR (282 MHz, THF-d_8): δ −28.7. Anal. Calcd (found) for C$_{20}$H$_{24}$F$_6$N$_2$Ni: C, 51.65 (51.13); H, 5.20 (5.79); N, 6.02 (5.99).

Preparation of [(dtbpy)Ni(CF$_2$CF$_3$)$_2$] (2). This complex was obtained from [NiBr$_2$(dme)] (0.201 g, 0.65 mmol), dtbpy (0.181 g, 0.67 mmol), CsF (0.450 g, 2.96 mmol), Me$_3$SiCF$_2$CF$_3$ (0.502 g, 2.61 mmol), THF (10 mL), and DMF (8 mL) in the same manner as that for [Ni(CF$_3$)$_2$(dtbpy)]. The complex was isolated as an orange powder (0.071 g, 0.13 mmol, 20%). Suitable single crystals for X-ray analysis were obtained by recrystallization from THF/pentane at −35 °C. ^{1}H NMR (300 MHz, THF-d_8): δ 8.61 (d, J = 6.3 Hz, 2H, dtbpy), 8.17 (d, J = 1.8 Hz, 2H, dtbpy), 7.66 (dd, J = 6.3, 1.8 Hz, 2H, dtbpy), 1.41 (s, 18H, CH$_3$). ^{13}C{^{1}H} NMR (126 MHz, THF-d_8): δ 165.5 (s, dtbpy), 155.6 (s, dtbpy), 153.1 (s, dtbpy), 124.3 (s, dtbpy), 119.5 (s, dtbpy), 36.3 (s, C(CH$_3$)$_3$), 30.2 (s, C(CH$_3$)$_3$). Although the signals assignable to CF$_2$CF$_3$ carbons were observed at 117−126 ppm, the chemical shifts for them were not able to be determined due to overlapping with the signals of dtbpy and complicated C−F couplings. ^{19}F NMR (282 MHz, THF-d_8): δ −79.0 (CF$_3$), −102.6 (CF$_2$). Anal. Calcd (found) for C$_{22}$H$_{24}$F$_{10}$N$_2$Ni: C, 46.67 (46.97); H, 4.28 (4.47); N, 4.96 (4.86). Dinuclear Ni complex 7 was obtained by recrystallization from CH$_2$Cl$_2$/hexane solution at −35 °C as orange crystals.

Preparation of [(dtbpy)NiMe$_2$] (3). dtbpy (0.358 g, 1.33 mmol) was added to Ni(acac)$_2$ (0.327 g, 1.27 mmol) dissolved in THF (10 mL). This suspension was stirred over 1 h at −20 °C. MeMgCl (3.0 M in ether, 869 uL, 2.61 mmol) was added dropwise to the suspension, which turned immediately dark green. After it was stirred for 1 h at −20 °C, the reaction mixture was passed through a glass filter. The volatiles of this resulting dark green solution were removed under reduced pressure. The residue was extracted with toluene and then filtered through a glass filter. After the removal of solvent, the residual solid was washed with pentane and dried in vacuo at 0 °C to give the desired [NiMe$_2$(dtbpy)] as a black powder (0.374 g, 1.06 mmol, 83%). ^{1}H NMR (300 MHz, benzene-d_6): δ 9.04 (d, J = 6.0 Hz, 2H, dtbpy), 7.43 (s, 2H, dtbpy), 6.72 (d, J = 6.0 Hz, 2H, dtbpy), 1.01 (s, 18H, CH$_3$), 0.98 (s, 6H, CH$_3$). ^{13}C{^{1}H} NMR (126 MHz, benzene-d_6): δ 158.3 (s, dtbpy), 154.8 (s, dtbpy), 147.6 (s, dtbpy), 123.3 (s, dtbpy), 116.4 (s, dtbpy), 34.9 (s, C(CH$_3$)$_3$), 29.9 (s, C(CH$_3$)$_3$), −4.5 (s, CH$_3$).

Electronic Structure Calculations. Quantum calculations were performed with the Gaussian09W software.[79] Unconstrained geometry optimizations were performed using the B3LYP exchange-correlation functional.[80,81] The m6-31G* basis set was used for nickel,[82] and the 6-31g* set was used for all other atoms. All calculations for optimized structures have been checked for the absence of imaginary frequencies. In all optimized structures, the singlet states were lower in energy than the triplet states (see the Supporting Information).

■ ASSOCIATED CONTENT

Ⓢ Supporting Information

Tables, figures, and CIF files giving crystallographic data for all newly determined structures and details of the structure calculations. This material is available free of charge via the Internet at http://pubs.acs.org.

■ AUTHOR INFORMATION

Corresponding Author
*E-mail: vicic@hawaii.edu.

Notes
The authors declare no competing financial interest.

■ ACKNOWLEDGMENTS

■ REFERENCES

(1) Carmona, E.; Gonzalez, F.; Poveda, M. L.; Atwood, J. L.; Rogers, R. D. *J. Chem. Soc., Dalton Trans.* **1981**, 769.
(2) Jacob, K.; Thiele, K. H.; Geyer, C.; Welde, G. *Z. Anorg. Allg. Chem.* **1980**, *462*, 177.
(3) Kohara, J.; Yamamoto, T.; Yamamoto, A. *J. Organomet. Chem.* **1980**, *192*, 265.
(4) Koo, K.; Hillhouse, G. L. *Organometallics* **1995**, *14*, 4421.
(5) Saito, T.; Uchida, Y.; Misono, A.; Yamamoto, A.; Morifuji, K.; Ikeda, S. *J. Am. Chem. Soc.* **1966**, *88*, 5198.
(6) Takahashi, S.; Suzuki, Y.; Sonogashira, K.; Hagihara, N. *J. Chem. Soc., Chem. Commun.* **1976**, 839.
(7) Tsou, T. T.; Kochi, J. K. *J. Am. Chem. Soc.* **1978**, *100*, 1634.
(8) Yamamoto, T.; Abla, M. *J. Organomet. Chem.* **1997**, *535*, 209.
(9) Yamamoto, T.; Nakamura, Y.; Yamamoto, A. *Bull. Chem. Soc. Jpn.* **1976**, *49*, 191.
(10) Yamamoto, T.; Yamamoto, A.; Ikeda, S. *J. Am. Chem. Soc.* **1971**, *93*, 3350.
(11) Klein, A.; Kaiser, A.; Sarkar, B.; Wanner, M.; Fiedler, J. *Eur. J. Inorg. Chem.* **2007**, 965.
(12) Dinjus, E.; Walther, D.; Kirmse, R.; Stach, J. *J. Organomet. Chem.* **1980**, *198*, 215.
(13) Kirmse, R.; Stach, J.; Dinjus, E.; Walther, D. *Z. Chem.* **1980**, *20*, 213.
(14) Walther, D.; Dinjus, E.; Ihn, W.; Schade, W. *Z. Anorg. Allg. Chem.* **1979**, *454*, 11.
(15) Chaudhury, N.; Kekre, M. G.; Puddephatt, R. J. *J. Organomet. Chem.* **1974**, *73*, C17.
(16) Davis, J. L.; Arndtsen, B. A. *Organometallics* **2011**, *30*, 1896.
(17) Han, R.; Hillhouse, G. L. *J. Am. Chem. Soc.* **1998**, *120*, 7657.
(18) Keim, W.; Berger, M.; Eisenbeis, A.; Kadelka, J.; Schlupp, J. *J. Mol. Catal.* **1981**, *13*, 95.
(19) Lin, B. L.; Clough, C. R.; Hillhouse, G. L. *J. Am. Chem. Soc.* **2002**, *124*, 2890.
(20) Matsunaga, P. T.; Hess, C. R.; Hillhouse, G. L. *J. Am. Chem. Soc.* **1994**, *116*, 3665.
(21) Matsunaga, P. T.; Mavropoulos, J. C.; Hillhouse, G. L. *Polyhedron* **1995**, *14*, 175.
(22) Yamamoto, A.; Morifuji, K.; Ikeda, S.; Saito, T.; Uchida, Y.; Misono, A. *J. Am. Chem. Soc.* **1965**, *87*, 4652.
(23) Yamamoto, T. *J. Chem. Soc., Chem. Commun.* **1978**, 1003.
(24) Yamamoto, T.; Kohara, T.; Osakada, K.; Yamamoto, A. *Bull. Chem. Soc. Jpn.* **1983**, *56*, 2147.
(25) Yamamoto, T.; Kohara, T.; Yamamoto, A. *Chem. Lett.* **1976**, 1217.
(26) Yamamoto, T.; Kohara, T.; Yamamoto, A. *Bull. Chem. Soc. Jpn.* **1981**, *54*, 2161.
(27) Yamamoto, T.; Kohara, T.; Yamamoto, A. *Bull. Chem. Soc. Jpn.* **1981**, *54*, 1720.
(28) Yamamoto, T.; Yamamoto, A. *Chem. Lett.* **1978**, 615.
(29) Bialek, M.; Cramail, H.; Deffieux, A.; Guillaume, S. M. *Eur. Polym. J.* **2005**, *41*, 2678.
(30) Kaul, E.; Senkovskyy, V.; Tkachov, R.; Bocharova, V.; Komber, H.; Stamm, M.; Kiriy, A. *Macromolecules* **2010**, *43*, 77.
(31) Kiriy, A.; Senkovskyy, V. *Polym. Prepr.* **2010**, *51*, 233.
(32) Senkovskyy, V.; Beryozkina, T.; Bocharova, V.; Tkachov, R.; Komber, H.; Lederer, A.; Stamm, M.; Severin, N.; Rabe, J. P.; Kiriy, A. *Macromol. Symp.* **2010**, *291−292*, 17.
(33) Senkovskyy, V.; Beryozkina, T.; Komber, H.; Lederer, A.; Stamm, M.; Kiriy, A. *Polym. Prepr.* **2008**, *49*, 630.
(34) Senkovskyy, V.; Kaul, E.; Tkachov, R.; Komber, H.; Stamm, M.; Kiriy, A. *Polym. Prepr.* **2010**, *51*, 367.
(35) Senkovskyy, V.; Tkachov, R; Beryozkina, T.; Komber, H.; Oertel, U.; Horecha, M.; Bocharova, V.; Stamm, M.; Gevorgyan, S. A.; Krebs, F. C.; Kiriy, A. *J. Am. Chem. Soc.* **2009**, *131*, 16445.
(36) Tkachov, R.; Senkovskyy, V.; Horecha, M.; Oertel, U.; Stamm, M.; Kiriy, A. *Chem. Commun.* **2010**, *46*, 1425.
(37) Tkachov, R.; Senkovskyy, V.; Komber, H.; Sommer, J.-U.; Kiriy, A. *J. Am. Chem. Soc.* **2010**, *132*, 7803.

(38) Tkachov, R.; Senkovskyy, V.; Oertel, U.; Synytska, A.; Horecha, M.; Kiriy, A. *Macromol. Rapid Commun.* **2010**, *31*, 2146.

(39) Yamamoto, T.; Konagaya, S.; Yamamoto, A. *J. Polym. Sci., Polym. Lett. Ed.* **1977**, *15*, 729.

(40) Yamamoto, T.; Konagaya, S.; Yamamoto, A. *J. Polym. Sci., Polym. Lett. Ed.* **1978**, *16*, 7.

(41) Durandetti, M.; Perichon, J. *Synthesis* **2004**, 3079.

(42) Budnikova, Y. G.; Kargin, Y. M.; Sinyashin, O. G. *Mendeleev Commun.* **1999**, 193.

(43) Budnikova, Y. H.; Perichon, J.; Yakhvarov, D. G.; Kargin, Y. M.; Sinyashin, O. G. *J. Organomet. Chem.* **2001**, *630*, 185.

(44) de França, K. W. R.; Navarro, M.; Leonel, E.; Durandetti, M.; Nedelec, J.-Y. *J. Org. Chem.* **2002**, *67*, 1838.

(45) Gosmini, C.; Nedelec, J. Y.; Perichon, J. *Tetrahedron Lett.* **1999**, *41*, 201.

(46) Morimoto, H.; Tsubogo, T.; Litvinas, N. D.; Hartwig, J. F. *Angew. Chem., Int. Ed.* **2011**, *50*, 3793.

(47) Ball, N. D.; Gary, J. B.; Ye, Y.; Sanford, M. S. *J. Am. Chem. Soc.* **2011**, *133*, 7577.

(48) Loy, R. N.; Sanford, M. S. *Org. Lett.* **2011**, *13*, 2548.

(49) Wang, X.; Truesdale, L.; Yu, J.-Q. *J. Am. Chem. Soc.* **2010**, *132*, 3648.

(50) Cho, E. J.; Senecal, T. D.; Kinzel, T.; Zhang, Y.; Watson, D. A.; Buchwald, S. L. *Science* **2010**, *328*, 1679.

(51) Dubinina, G. G.; Brennessel, W. W.; Miller, J. L.; Vicic, D. A. *Organometallics* **2008**, *27*, 3933.

(52) Dubinina, G. G.; Furutachi, H.; Vicic, D. A. *J. Am. Chem. Soc.* **2008**, *130*, 8600.

(53) Dubinina, G. G.; Ogikubo, J.; Vicic, D. A. *Organometallics* **2008**, *27*, 6233.

(54) McReynolds, K. A.; Lewis, R. S.; Ackerman, L. K. G.; Dubinina, G. G.; Brennessel, W. W.; Vicic, D. A. *J. Fluorine Chem.* **2010**, *131*, 1108.

(55) Oishi, M.; Kondo, H.; Amii, H. *Chem. Commun.* **2009**, 1909.

(56) Knauber, T.; Arikan, F.; Roeschenthaler, G.-V.; Goossen, L. J. *Chem. Eur. J.* **2011**, *17*, 2689.

(57) Tomashenko, O. A.; Escudero-Adan, E. C.; Martinez, B. M.; Grushin, V. V. *Angew. Chem., Int. Ed.* **2011**, *50*, 7655.

(58) Cundy, C. S.; Green, M.; Stone, F. G. A. *J. Chem. Soc. A* **1970**, 1647.

(59) Gasafi-Martin, W.; Oberendfellner, G.; von, W. K. *Can. J. Chem.* **1996**, *74*, 1922.

(60) Hoberg, H.; Guhl, D. *J. Organomet. Chem.* **1989**, *378*, 279.

(61) Klein, A.; Feth, M. P.; Bertagnolli, H.; Zalis, S. *Eur. J. Inorg. Chem.* **2004**, 2784.

(62) Cacace, F.; Caronna, S. *J. Am. Chem. Soc.* **1967**, *89*, 6848.

(63) Martinez-Salvador, S.; Fornies, J.; Martin, A.; Menjon, B. *Angew. Chem., Int. Ed.* **2011**, *50*, 6571.

(64) Martinez-Salvador, S.; Fornies, J.; Martin, A.; Menjon, B. *Chem. Eur. J.* **2011**, *17*, 8085.

(65) Loutfy, R. O.; Loutify, R. O. *Can. J. Chem.* **1976**, *54*, 1454.

(66) Kieltsch, I.; Dubinina, G. G.; Hamacher, C.; Kaiser, A.; Torres-Nieto, J.; Hutchison, J. M.; Klein, A.; Budnikova, Y.; Vicic, D. A. *Organometallics* **2010**, *29*, 1451.

(67) Naumann, D.; Roy, T.; Tebbe, K. F.; Crump, W. *Angew. Chem.* **1993**, *105*, 1555.

(68) Naumann, D.; Tyrra, W.; Trinius, F.; Wessel, W.; Roy, T. *J. Fluorine Chem.* **2000**, *101*, 131.

(69) Grushin, V. V.; Marshall, W. J. *J. Am. Chem. Soc.* **2006**, *128*, 4632.

(70) Tomashenko, O. A.; Grushin, V. V. *Chem. Rev.* **2011**, *111*, 4475.

(71) Russell, J.; Roques, N. *Tetrahedron* **1998**, *54*, 13771.

(72) Tucci, G. C.; Holm, R. H. *J. Am. Chem. Soc.* **1995**, *117*, 6489.

(73) Per the request of a reviewer, the MOs of **3** were compared to those of a $[(bpy)Ni(CH_3)_2]$ analogue that was generated by substituting the fluorines of **1** with hydrogens. The MOs of the geometrically distorted dimethyl complex were destabilized relative to those of **3** (see the Supporting Information).

(74) Yang, D. S.; Bancroft, G. M.; Dignard-Bailey, L.; Puddephatt, R. J.; Tse, J. S. *Inorg. Chem.* **1990**, *29*, 2487.

(75) Hughes, R. P. *J. Fluorine Chem.* **2010**, *131*, 1059.

(76) Lichtenberger, D. L.; Elkadi, Y.; Gruhn, N. E.; Hughes, R. P.; Curnow, O. J.; Zheng, X. *Organometallics* **1997**, *16*, 5209.

(77) Glendening, E. D.; Reed, A. D.; Carpenter, J. E.; Weinhold, F. *NBO Version 3.1*.

(78) Noviandri, I.; Brown, K. N.; Fleming, D. S.; Gulyas, P. T.; Lay, P. A.; Masters, A. F.; Phillips, L. *J. Phys. Chem. B* **1999**, *103*, 6713.

(79) Frisch, M. J.;et al. *Gaussian 09 for Windows*, revision C.01; Gaussian, Inc.: Wallingford, CT, 2009. The full reference is provided in the Supporting Information.

(80) Becke, A. D. *J. Chem. Phys.* **1993**, *98*, 5648.

(81) Lee, C.; Yang, W.; Parr, R. G. *Phys. Rev. B* **1988**, *37*, 785.

(82) Mitin, A. V.; Baker, J.; Pulay, P. *J. Chem. Phys.* **2003**, *118*, 7775.